(10) Vincett, P. S.; Roberts, G. G. *Thin Solid Films* **1980**, *68*, 135.
(11) Roberts, G. G.; McGinnity, M.; Barlow, W. A.; Vincett, P. S. *Solid State Commun.* **1979**, *32*, 683.
(12) Batey, J.; Roberts, G. G.; Petty, M. C. *Thin Solid Films* **1983**, *99*, 283.
(13) Loyd, J. P.; Petty, M. C.; Roberts, G. G.; Lecomber, P. G.; Spear, W. E. *Thin Solid Films* **1983**, *99*, 297.
(14) Larkins, G. L., Jr.; Thompson, E. D.; Ortiz, E.; Burkhart, C. W.; Lando, J. B. *Thin Solid Films* **1983**, *99*, 277.
(15) Blinov, L. M.; Dubinin, N. V.; Miknev, L. V.; Yudin, S. G. *Thin Solid Films* **1984**, *120*, 161.
(16) Barraud, A.; Rosilio, C.; Raudel-Teixier, A. *Thin Solid Films* **1980**, *68*, 91.
(17) Miyashita, T.; Yoshida, H.; Matsuda, M. *Thin Solid Films* **1987**, *155*, L11.
(18) Boothroyd, B.; Delaney, P. A.; Hann, R. A.; Johnstone, R. A. W.; Lewith, A. *Br. Polym. J.* **1985**, *17*, 360.
(19) Miyashita, T.; Yoshida, H.; Murakata, T.; Matsuda, M. *Polymer* **1987**, *28*, 311.
(20) Miyashita, T.; Yoshida, H.; Itoh, H.; Matsuda, M. *Nippon Kagaku Kaishi* **1987**, 2169.
(21) Barraud, A.; Rosilio, C.; Ruaudel-Teixier, A. *J. Colloid Interface Sci.* **1977**, *62*, 509.
(22) Naegele, D.; Lando, J. B.; Ringsdorf, H. *Macromolecules* **1977**, *10*, 1339.
(23) Shigehara, K.; Hara, M.; Nakahama, H.; Miyata, S.; Murata, Y.; Yamada, A. *J. Am. Chem. Soc.* **1987**, *109*, 1237.
(24) Mumby, S.; Swalen, J. D.; Rabolt, J. F. *Macromolecules* **1986**, *19*, 1054.
(25) Hodge, P.; Khoshdel, E.; Tredgold, R. H.; Vickers, A. J.; Winter, C. S. *Br. Polym. J.* **1985**, *17*, 368.
(26) Murakata, T.; Miyashita, T.; Matsuda, M. *Macromolecules* **1988**, *21*, 2730.
(27) Gabrielli, G.; Puggelli, M.; Baglioni, P. *J. Colloid Interface Sci.* **1981**, *86*, 485.
(28) Gabrielli, G.; Maddii, A. *J. Colloid Interface Sci.* **1978**, *64*, 19.
(29) Gabrielli, G.; Balglioni, P.; Maddii, A. *J. Colloid Interface Sci.* **1979**, *79*, 268.
(30) Yokoyama, M.; Tamamura, T.; Atsumi, M.; Yoshimura, M.; Shirota, Y.; Mikawa, H. *Macromolecules* **1975**, *9*, 101.
(31) Okamoto, K.; Yano, A.; Kusabayashi, S.; Mikawa, H. *Bull. Chem. Soc. Jpn.* **1974**, *47*, 749.

Entanglement Scaling in Polymer Melts and Solutions

Tom A. Kavassalis* and Jaan Noolandi

Xerox Research Centre of Canada, 2660 Speakman Drive, Mississauga, Ontario L5K 2L1, Canada. *Received April 15, 1988; Revised Manuscript Received December 14, 1988*

ABSTRACT: In this paper, we develop several universal scaling laws for molecular entanglements in polymer melts and solutions and compare our predictions against experimental data. The model used here is a generalization of our previous work where entanglements were described by a universal topological parameter, $\tilde{N}$. Predictions for the mean entanglement spacing as a function of the polymer chemical and structural properties were found to be in good agreement with experimental data. The model also predicts a transition from entangled chains to unentangled chains at a degree of polymerization, N_c, that correlates well with values determined from steady-state compliance measurements. The model transition is shown to be analogous to the liquid–gas critical point predicted by the van der Waals equation of state and leads directly to departures from the reptation theory scaling laws for shear viscosity without invoking new mechanisms. Scaling laws are developed for entanglements in solution and are in good agreement with experimental data. Predictions made for the onset of entanglement effects in solution closely parallel earlier work on chain overlap by de Gennes. A relationship between the overlap threshold density and entanglement threshold density is predicted in terms of the parameter $\tilde{N}$.

1. Introduction

The reptation or tube model of de Gennes[1] and Doi and Edwards[2] has provided the framework for understanding many of the transport and mechanical properties of entangled polymers both in the melt and in solution. The model, which builds on earlier work on rubber elasticity,[3] assumes the presence of a certain average number of entanglements per polymer chain. Using the noncrossability of chains, a kinetic equation was developed to describe the evolution of the polymer conformation. This equation described the polymer as evolving in a tube formed by the surrounding chains. The degree of entanglement amongst chains was described by a phenomenological parameter, N_e, which represents the mean number of polymer skeletal bonds between entanglements. A relationship between N_e and the polymer properties was not given.

A quantitative description of molecular entanglements and their interactions is still one of the more challenging problems in polymer physics. The difficulty of topological classification of entanglements is compounded by the mathematical difficulty of describing the entanglement interaction. A "first-principles" derivation of the reptation theory perhaps hinges on developments along these lines. Such a theory would merge continuously with the Rouse theory for short chains and also describe the transition from the highly entangled state to the unentangled state. A missing element thus far has been a mathematical criterion for describing entanglements.

Despite the absence of a unifying theory, significant progress has been made toward understanding the shortcomings of the reptation theory in the transition region. For example, Graessley[4] has shown that the tube renewal process can effectively compete with reptation for finite length chains. Improved agreement between experiment and theory was observed when a tube renewal effect was considered. The original tube renewal model, however, lacks self-consistency. For example, the nonreptative corrections applied to the test chain are derived assuming bare reptation dynamics for the surrounding chains. This feature makes the model unsuitable for describing the dynamics near the transition. Perhaps an iterative procedure would improve the model in this regime.

Doi[5] recognized that tube length fluctuations can be important for finite length chains and proposed a model for incorporating this effect in the reptation theory. Doi's solution of the length fluctuation model included a variational parameter that could quantitatively account for departures from the $\eta_0 \sim M^3$ power law. Des Cloizeaux's[6] in-depth analysis of a similar model concluded that the effect of length fluctuations is not as large as Doi had predicted.

Recently, Hess[7] has taken a more fundamental approach. Starting with a Fokker–Planck equation, for the phase space distribution function for all polymer segments,

0024-9297/89/2222-2709$01.50/0

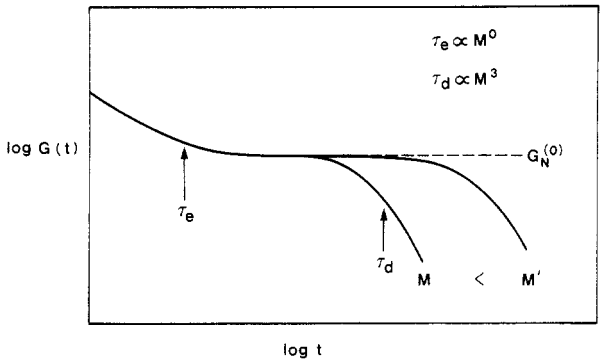

Figure 1. Schematic illustration of the stress relaxation modulus, $G(t)$, of high molecular weight polymer, $M > M_c$, as a function of time, t. The short-time behavior ($t < \tau_e$) involves local rearrangement of polymer bonds and is independent of chain molecular weight, M. The long-time behavior ($t > \tau_d$) corresponds to viscous flow, and there is a strong molecular weight dependence. At intermediate times, there is a rubbery plateau, which is the signature of the transient network of entanglements.

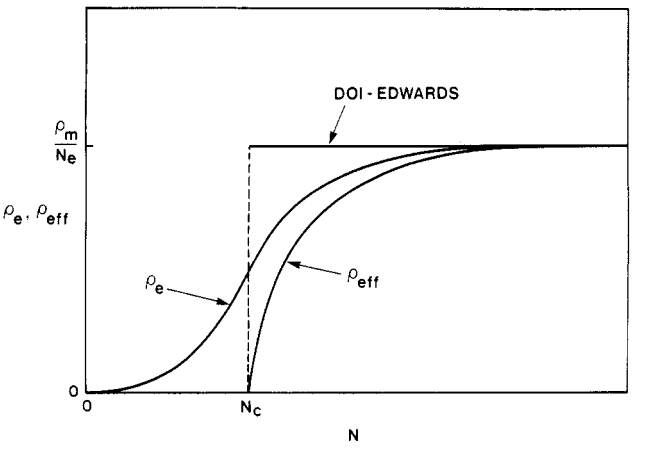

Figure 2. Schematic illustration of the density of entanglements as a function of degree of polymerization, N. For large N, the density of entanglements is independent of N, corresponding to a constant mean entanglement spacing, N_e. At very small N, the density of entanglements is zero since short chains are not likely to be entangled. For intermediate length chains, a transition region should exist where the chains are weakly entangled relative to the long-chain limit. The curve labeled ρ_e may correspond to the actual density of entanglements, although this is difficult to define without a criterion for what an entanglement is. The curve labeled ρ_{eff} may correspond to the density of those entanglements that are long lived relative to a microscopic chain rearrangement time. This density would not, for example, include the entanglements involving chain ends than can be undone in a relatively short time. With this specific criterion, we would expect ρ_{eff} to fall identically to zero at N_c. The solid horizontal curve represents the conventional assumption used in polymer dynamic models.

he invoked a projection operation to derive a formal expression for the diffusion coefficient. By decomposing the propogator into longitudinal and transverse components and including the excluded volume interaction, Hess was able to express the diffusion coefficient in terms of reptative and nonreptative contributions. Scaling theory results, which lack numerical coefficients, were ultimately employed to complete the theory. The entanglement parameter, N_c, defined as the critical degree of polymerization for entanglements, appears again as an adjustable parameter.

It is now well-known that chain entanglements can profoundly effect the viscoelastic relaxation of linear chain polymer melts.[8] For example, the stress relaxation modulus of high molecular weight polymers, with narrow molecular weight distributions, develops a plateau at times intermediate to the glassy and terminal response regimes (Figure 1). This rubbery plateau is the signature of the transient entanglement network that exists in a melt prior to viscous flow and by anology to the theory of rubber elasticity can be related to the mean number of polymer bonds between entanglement points, N_e, as follows

$$G_N^\circ = \frac{\rho_m k_B T}{N_e} \tag{1}$$

where ρ_m is the monomer number density, and $k_B T$ is the Boltzmann temperature. Equation 1 is routinely used to extract the value of N_e from experimental stress–relaxation measurements. In practice, the plateau region is only observed for high molecular weight, monodisperse samples.

The magnitude of the plateau modulus, G_N°, is a characteristic of the polymer under investigation, and most linear chain polymers fall in the range 0.2–2 MPa. While G_N° varies from one polymer to the next, several properties are known to be universal.[9] For example, the quantity $G_N^\circ/k_B T$ is insensitive to temperature. This is consistent with the view that N_e is purely a geometrical property of the entangled chains. Also, for sufficiently high molecular weight, G_N° is independent of molecular weight. The variation in G_N° values, therefore, must originate in the structural or conformational differences between polymers which determine the extent to which entanglements will form. Several researchers have attempted to correlate the chemical/structural properties of polymers to mechanical properties, such as the plateau modulus, and have met with varying degrees of success.[10-14] The merit of such undertaking is obvious. They will ultimately reduce the number of free parameters in the original reptation theory by rendering N_e to computation. More importantly, they will lead to an improved description of the entangled state, which may further aid the development of dynamic models.

One important requirement of an entanglement theory is a criterion for the presence of entanglements. In a polymer melt, for example, the degree of entanglement (or lack of entanglements) should be computable from the conformational properties of the chains. We conjecture that the situation is as we depict in Figure 2. The density of entanglements, ρ_e, is independent of chain length for long chains and then shows a chain length dependence as we approach N_c. For sufficiently short chains, chain entanglement is less likely and ρ_e should vanish. The ρ_e curve is, however, difficult to define without first prescribing a criterion for whether or not a group of conformations are to be considered an entanglement. We can, however, consider a subset of entanglement interactions where one is only interested in those entanglements that will persist longer than an appropriate microscopic time. For example, the entanglements that involve the tails of a polymer will evolve and disappear on a faster time scale than those involving a polymer midsection. The density of effective entanglements, defined in this manner, will fall identically to zero below a critical degree of polymerization, which we donate by N_c.

Recently,[15,16] we have proposed a description of entanglements that contains the features that are described above. The model encompasses a new definition of entanglements in terms of the mean number of neighboring polymer segments required to restrict the lateral degrees of freedom of a chain. This is in sharp contrast to the conventional view of entanglements involving well-defined loops or knots between pairs of chains. The model leads to specific predictions on how the unentangled state is approached as chain length is shortened. It also describes the manner in which N_e and N_c will depend on the polymer

characteristic ratio, C_∞, bond length, l, monomer molecular weight, μ_m, and the overall density, ρ.

The purpose of the present paper is to develop scaling laws for the entanglement parameters of polymer melts and solutions. In section 2, we review our entanglement theory for monodisperse polymer melts and characterize the transition at N_c. The anology to other "phase transitions" is explored, and the universality is identified. In section 3, we compare our entanglement predictions against current rheological data for a variety of polymers. In particular, we compare our predictions for N_e, N_c, and the transition region against experimental data. In section 4, we generalize the entanglement theory to polymer solutions and discuss entanglement scaling laws first for general solvents and then for special limiting cases.

2. Entanglement Theory

Traditionally, molecular entanglements are described as pairwise topological interactions amongst inpenetrable chains, which can involve various configurations ranging from winding loops to perhaps even knots. While in principle these sorts of geometries can exist, in a dense system of long chains, a simple scaling analysis reveals that the number of polymer segments within an entanglement volume, defined by a sphere with diameter $\sim C_\infty^{1/2}N_e^{1/2}l$ surrounding a segment of a test chain with N_e skeletal bonds, is of the order $N_e^{1/2} \sim 10$–20 and not simply 2 or 3. This suggests an alternative view of topological interactions and forms the basis for our entanglement theory.[15,16]

We have defined a mean entanglement as consisting of a sufficient number of neighboring polymer chain segments that on average restrict the lateral degrees of freedom of a test chain. This picture of an entanglement does not attempt to enumerate the complicated geometries of the test chain and surrounding chains and therefore, in some sense, represents an average or composite entanglement. Entanglements of the traditional sort, involving fewer intertwined or knotted chains, can exist within this composite entanglement, and the number of neighboring chains should be a sufficient measure of the probability of this situation occurring.

In Figure 2 we suggested that the density of the effective entanglements is not independent of chain length. We now rationalize this figure with the following thought experiment. Imagine a system of entangled polymer chains with degree of polymerization N. Labeling one chain as the test chain, we inscribe a subsection of the chain, with N_e bonds, in a sphere with diameter $C_\infty^{1/2}N_e^{1/2}l$. The various polymer segments within this sphere including the test chain segment constitute the entanglement in our view. Now imagine rescaling the lengths of all polymers in this system but preserving the overall density by cutting all chains at their midpoints. Some of the cuttings will occur within the imaginary sphere with probability proportional to $1/N$. The loose ends produced by our microscopic surgeon are not expected to contribute to the formation of long-lived or *effective* entanglements. In order to recover our original definition of an entanglement, that is, consisting of a certain number of constraining chains, we must enlarge the imaginary sphere by the appropriate amount, hence the chain length dependence of ρ_{eff} in Figure 2.

In this picture, therefore, we have defined an *effective entanglement* by the presence of a certain number of *nontail* neighboring polymer segments. If we, therefore, continue the cutting process, of our thought experiment, we will eventually reach an unentangled state. In the unentangled state, any sphere with diameter less than $C_\infty^{1/2}N^{1/2}l$ will contain fewer than the required number of nontail segments to form an effective constraint. This description of entanglements leads to the abrupt transition at N_c for ρ_{eff} depicted in Figure 2. To understand the origin of this transition, recall that if we enlarge the imaginary sphere, in order to incorporate more nontail segments, there is a finite probability of also incorporating the tail segments of some of the nontails in the sphere. This will require a further enlargement of the sphere, which leads to an accelerated transition.

The mathematical framework for describing entanglements in the manner described above is as follows.[15,16] The mean number of skeletal bonds between entanglement points, N_e, is related to a universal constant, $\tilde{N}$, called the coordination number, and the chain dimension, N, according to

$$\tilde{N} + 1 = \frac{\pi\psi}{6}N_e^{1/2}(1 - N_e/N) \tag{2}$$

where ψ is a dimensionless constant containing the material parameters

$$\psi = \frac{\rho C_\infty^{3/2} l^3}{\mu_m} \tag{3}$$

In the last formula, ρ is the polymer mass density, C_∞ is the characteristic ratio, l is the mean skeletal bond length, and μ_m is the monomer mass per skeletal bond. The system of interest here consists of Gaussian monodisperse chains of degree of polymerization N without hard core excluded volume interactions amongst the chains. The second term of the right-hand side of eq 2 arises from the polymer tails, which we exclude from contributing to the entanglement network in much the same way Flory excluded dangling tails from contributing to the elastic modulus of a rubber. The form of eq 2 is similar to Flory's expression[17] for the elastic modulus

$$G = \frac{\rho k_B T}{M_c}\left(1 - \frac{2M_c}{M}\right) \tag{4}$$

where here M_c is the molecular weight between cross-links and M is the original material molecular weight.

The parameter $\tilde{N}$, in eq 2, is the mean number of polymer segments that contribute to the formation of an entanglement, as discussed previously. We have conjectured that, while N_e may vary from one system to the next, the number of polymers involved in forming a "mean" entanglement should be universal. An argument for the universality of $\tilde{N}$ is as follows. Consider first a subsection of an ideal random walk polymer ($C_\infty = 1$) which contains N_e bonds where N_e is the appropriate mean entanglement spacing for this system. Inscribe this polymer segment in a sphere with diameter $D_e = N_e^{1/2}l$, and begin adding other chains. The probability that this segment becomes surrounded by the other chains in a manner that restricts its lateral movements will increase with the addition of other chains but will level off at a certain number, $\tilde{N}$, at which point we stop adding chains. For a real polymer segment with the same number of bonds, the sphere diameter would be larger than the pure random walk chain due to bond correlations, $D_e = C_\infty^{1/2}N_e^{1/2}l$. Therefore, transforming the test chain and the $\tilde{N}$ other chains into chains with characteristic ratio C_∞, but retaining the gross topology established for the ideal chains, we see that we can accommodate additional chains within the test chain's volume. The total number of chains added will be governed by the polymer density. The additional chains added will increase the degree of entanglements by further constraining the test chain. Therefore, a small value of N_e should be chosen

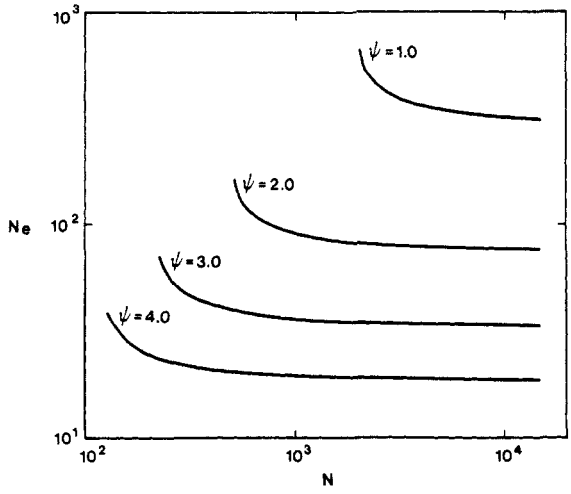

Figure 3. Mean entanglement spacing, N_e, versus degree of polymerization, N, for a melt computed by using eq 8 with $\tilde{N}$ = 8.1 and several values of $\psi = \rho C_\infty^{3/2} l^3/\mu_m$. For large N, the curves approach their respective asymptotic values $N_e(\infty) = [6(\tilde{N}+1)/\pi\psi]^2$. The entanglement is defined here as consisting of $\tilde{N}$ neighboring chain segments excluding tail segments. This leads to an increase in N_e with shortening of the chains and an abrupt transition to unentangled chains at $N_c = 3^5[(\tilde{N}+1)/\pi\psi]^2$.

to define a single entanglement. This smaller value of N_e will be determined by that volume that once again contains $\tilde{N}$ other chains. The differences between one polymer and another enter through their respective values of ϕ. In the next section, we demonstrate this point by comparing our predictions with recent experimental data.

Equation 2 exhibits the properties proposed in our thought experiments. For long chains, the second term in eq 2 vanishes, and the density of entanglements approaches a constant value

$$\rho_{eff}(\infty) = \frac{\rho_m}{N_e(\infty)} = \frac{(\pi\psi)^2\rho_m}{[6(\tilde{N}+1)]^2} \tag{5}$$

where ρ_m is the monomer number density. Also, for any finite value of N, the density of entanglements is lower than the asymptotic value. Finally, a transition is predicted[15,16] and occurs at a critical value of $N = N_c$ that satisfies

$$N_c = 3N_e(N_c) \tag{6}$$

$$N_c = \frac{27}{4}N_e(\infty) \tag{7}$$

The exact solution of eq 2, which was not previously reported, is

$$N_e = (4/3)N\cos^2[(1/3)\arccos(N_e/N)^{1/2} + 4\pi/3] \tag{8}$$

and was used to generate the plots of N_e versus N in Figure 3.

The nature of this model transition is in itself an interesting problem. Both above and below N_c, the chain conformations are Gaussian with the same conformational parameters, C_∞, and density, ρ. Therefore, both above and below N_c, we have purely disordered systems with one essential difference. In the entangled regime, conformational correlations are longer lived because of the topological constraints imposed by the surrounding chains. This statement holds even though the polymer conformations may be evolving in a highly cooperative manner in the transition region. We recognize, therefore, that this is analogous to the liquid–gas critical point where the liquid and gas have essentially the same type of disorder, but positional correlations in the liquid are longer lived. The difference, of course, vanishes at the critical point.

The analogy to the liquid–gas critical point can be exploited further. By squaring both sides of eq 2 and rearranging terms, we can write

$$N_e^3 - (2N)N_e^2 + N^2N_e - \left[\frac{6(\tilde{N}+1)}{\pi\psi}\right]^2 N^2 = 0 \tag{9}$$

which has the same form as the familiar van der Waals equations of state for a gas

$$V^3 - \left(b + \frac{RT}{p}\right)V^2 + \frac{a}{p}V - \frac{ab}{p} = 0 \tag{10}$$

where a and b are positive constants. The critical properties of eq 9 can therefore be termed classical or mean field. Indeed, if we expand the solution of eq 2, in eq 8, around the "critical" point, we find the classical $\delta = {}^1/_2$ exponent for N_e as follows:

$$\frac{N_e(N) - N_e(N_c)}{2N_c} = \frac{-1}{3^{1/2}}\left(\frac{N - N_c}{N_c}\right)^{1/2} \tag{11}$$

We can similarly write a law of corresponding states, that is, a law free of parameters, by scaling N and N_e as follows

$$N_e^* = N_e/N_e(N_c) \tag{12}$$

$$N^* = N/N_c \tag{13}$$

and then obtain

$$N_e^{*3} - 6N^*N_e^{*2} + 9N^{*2}N_e^* - 4N^{*2} = 0 \tag{14}$$

It has long been recognized that mean field theories are generally poor in $d < 4$ dimensions.[18] For example, the experimentally measured exponent for the liquid–gas critical point is $\delta = 0.33$. The discrepancy between mean field theory and experiments has been attributed to the absence of fluctuation phenomena which become more important near the transition. The anology to the liquid–gas system, however, suggests that perhaps the more advanced renormalization group techniques can be applied to polymer entanglements as well. In section 3a, we compare the predictions of eq 2 against experimental data away from the critical point, where the mean field assumptions should be of no consequence.

3. Rheological Correlations

In this section, we compare the predictions of our entanglement theory against experimental rheological data for various linear chain polymers obtained from the literature. The section is organized into three parts dealing with the long-chain limit (strongly entangled), intermediate length chains (weakly entangled), and chains at the unentangled threshold. In all three cases, we consider monodisperse materials only. The generalizations to polydisperse systems are straightforward and can be found in ref 16.

3a. The Long-Chain Limit. First we begin by considering polymer chains that are far away from the transition region, that is, with $N \gg N_e$. In this limit, eq 2 reduces to

$$\tilde{N} + 1 = \left(\frac{\pi\rho C_\infty^{3/2} l^3}{6\mu_m}\right)N_e^{1/2} \tag{15}$$

where we have substituted in the definition of ψ from eq 3. On the right-hand side, we have a particular combination of material specific parameters which, according to our model, should combine to give a pure number. Therefore, a critical test of theory is to determine the

Table I
Polymer Structural and Entanglement Properties Compared against Entanglement Models[a]

	ρ, g/cm^3	10^8e, cm	$\mu_m N_a$, g	C_∞	N_e	$\tilde{N}+1$	K	n_t
polystyrene	1.007	1.54	52	9.4	259	10.3	10.2	19.7
poly(α-methylstyrene)	1.04	1.54	59	10.1	173	8.59	8.23	16.4
polybutadiene (high cis)	0.9	1.47	13.5	4.9	174	9.53	10.4	18.2
polyisobutylene	0.89	1.54	28	6.2	252	8.95	10.5	17.1
polyisoprene (high cis)	0.9	1.47	17	5.3	238	9.95	11.3	19
hydrogenated polyisoprene	0.854	1.54	17.5	6.8	84	9.16	7.83	17.5
poly(vinyl acetate)	1.14	1.54	43	9	162	10.5	9.22	20
polybutadiene, χ_{12} = 0.08	0.896	1.47	14.1	5.1	101	7.59	7.91	14.5
polybutadiene, χ_{12} = 0.43	0.9	1.47	17.2	6.1	108	8.48	8.12	16.2
polybutadiene, χ_{12} = 0.99	0.883	1.54	26.7	7	160	8.90	9.03	17
polyethylene	0.802	1.54	14	7.4	52.6	9.27	6.91	17.7
hydrogenated polybutadiene, χ_{12} = 0.43	0.832	1.54	17.8	6.4	95.5	8.53	7.93	16.3
hydrogenated polybutadiene, χ_{12} = 0.99	0.819	1.54	27.7	5.5	386	8.64	11.8	16.5
average						9.1	9.2	17.4
std dev						8%	16%	8%

[a] Data taken from ref 14. $\tilde{N}+1$ is from the present work (eq 15) and ref 15 and 16. K is from Graessley and Edwards[12] (eq 18). n_t is from Lin[14] (eq 19).

accuracy of this relation. Before doing so, we review some of the predictions of previous, dimensional analysis approaches to the same problem for the purposes of comparison.

Graessley and Edwards[12] argued that since G_N°/k_BT is a measure of the concentration of network junctions, it should therefore be viewed as some sort of interaction density. They then put forth the hypothesis that G_N°/k_BT should depend on υ, the density of chains, and L, the length of the chains. In other words, they identified L as the relevant length scale for the interaction and υ as the density of such interactions. Since G_N°/k_BT has dimensions of (length)$^{-3}$ and the product υL has dimensions of (length)$^{-2}$, they introduced an additional length scale $l' = C_\infty l$, the Kuhn length, to form dimensionless quantities.

With the previous argument, Graessley and Edwards[12] proposed that G_N° should be related to the relevant quantities by a universal function, F,

$$\frac{G_N^\circ l'^3}{k_BT} = F(\upsilon L l'^2) \tag{16}$$

The nature of the universal function was deduced by requiring that $G_N^\circ l'^3/k_BT$ scale with polymer density according to

$$\frac{G_N^\circ l'^3}{k_BT} = \rho^a \tag{17}$$

where the value of a is known to be in the range 2.0–2.3 from experiments.[9] Choosing a value of $a = 2$, substituting the definition of $\upsilon = \rho/(\mu_m N)$ and $L = Nl$, and casting eq 16 into a form similar to eq 15, we obtain their prediction that

$$K = \left[\frac{\rho C_\infty l^3}{\mu_m}\right]^{1/2} N_e^{1/2} \tag{18}$$

where K should be a universal constant. The constant K does not appear to render itself to an interpretation such as $\tilde{N}$.

The difference between eq 15 and 18 stems from the choice of length scales. When υ, L, and l are chosen as relevant quantities for scaling, an important intermediate length scale is neglected, the length scale of entanglements. For example, the density of polymer chains in volume V, which is much larger than the polymers radius of gyration, is ρ_m/N, where ρ_m is the monomer density. The number of polymer chains in this volume is $V\rho_m/N$. In a volume that is small compared to the chain's radius of gyration, such as the volume of an entanglement, the number of polymer segments is proportional to $C_\infty^{3/2}N_e^{1/2}$. So, if the entanglement length scale is chosen as the relevant length scale, we can arrive at eq 15 by an dimensional analysis argument.

Recently, Lin[14] has proposed a universal relation between the entanglement spacing (N_e) and the material parameters that closely parallel our results for the long-chain limit. Lin's argument, which is also based on dimensional analysis, recognizes the importance of the entanglement length scale. He constructed a dimensionless quantity, n_t, which has the form

$$n_t = \rho\frac{N_a}{M_e}\left(C_\infty\frac{M_e}{m}l^2\right)^{3/2} \tag{19}$$

where m is the monomer molecule weight per skeletal bond, M_e is the molecular weight between entanglements, and N_a is Avogadro's number. The interpretation of n_t is essentially the same as $\tilde{N}+1$, that is, the number of polymer strands per entanglement volume. Noting that $M_e/m = N_e$ and $M_e/N_a = N_e\mu_m$, Lin's equation reduces to eq 15, apart from a factor of $\pi/6$. The factor of $\pi/6$ originates from the choice of a spherical entanglement volume in our model and a cubical volume in Lin's model. Privalko[11] had earlier deduced on an equation similar to eq 15 and 19 by using dimensional analysis. Others still have used statistical approaches to establish correlations between entanglement parameters and molecular quantities. For example, Aharoni[13] has inferred a correlation between the critical chain length for entanglements and the characteristic ratio of the form

$$N_c \propto C_\infty^2 \tag{20}$$

The fact that the correlations were found to be weak is not too surprising given that the monomer mass, bond length, and polymer density were omitted from the relation.

In Table I, we have reproduced[12,14] a compilation of experimentally determined values of C_∞ and N_e for a variety of polymers along with their respective values of ρ and l. Columns 6, 7, and 8 contain the computed values of $\tilde{N}+1$, K, and n_t according to eq 15, 18, and 19, respectively. Since $\tilde{N}+1$ and n_t are essentially the same, apart from a factor of $\pi/6$, we will only discuss the former in the remainder of this section.

The mean values of $\tilde{N}+1$ and K are 9.1 ± 0.8 and 9.2 ± 1.5, respectively. The error reported here is the standard deviation and is significantly smaller in the $\tilde{N}+1$ values. The standard deviation as a percentage of the mean is 8%

for $\tilde{N}+1$ and n_t and 16% for K. In the original work by Graessley and Edwards,[12] the standard deviation was reported to be 30%. This value refers to a relation that is essentially the square of eq 18. Since the left-hand sides of eq 15, 18, and 19 are pure numbers, any operation such as squaring, cubing, etc., also leaves a pure number. It is therefore necessary to choose forms that have a common power of the more uncertain variable, which in this case is N_e. Lin[14] compared his results against the Graessley–Edwards[12] results without taking this into account. The scatter in $\tilde{N}+1$ values is surprisingly small given that experimental errors in N_e values are typically ±10%. The values of N_e are also within the physical limits imposed by its interpretation. Too large (~100) or too small (~1) a number would have been suspect.

While the data in Table I suggest that the universal relation for N_e, C_∞, l, μ_m, and ρ predicted in eq 15 is in better agreement with experimental data than the prediction in eq 18, an apparent discrepancy exists. Equation 18 was constructed to agree with the experimentally known scaling relation in solutions, $G_N^\circ \propto \rho^2$. No such constraints were imposed in deriving eq 15. The data in Table I span a fairly wide range of polymer densities from 0.802 for polyethylene to 1.14 for poly(vinyl acetate). Any systematic error in our scaling relation for N_e, such as an erroneous factor of ρ, should manifest itself with higher scatter in column 6 of Table I. The smaller scatter in $\tilde{N}+1$ values suggests that the scaling of N_e with density is probably not in error. In section 4, we generalize our entanglement model to various solution conditions and conclude that the density scaling law for N_e is different there.

3b. Intermediate Length Chains. Now we turn our attention to the transition regime where the degree of polymerization, N, is just above N_c. In this regime, we predict that polymer chains are weakly entangled as compared to longer chains and that the mean entanglement spacing, N_e, translates directly into departures from the reptation theory scaling laws as discussed below.

The maximum variation of N_e, that is, the ratio of the value of N_e in the long-chain limit to the value of N_e for chains of length N_c, can be computed as follows. The transition at N_c occurs when N_e has its maximum value, which we denote by $N_e(N_c)$. From eq 6 and 7, we have

$$N_c = 3N_e(N_c) \tag{21}$$

$$N_c = 27/4N_e(\infty) \tag{22}$$

and therefore

$$\frac{N_e(N_c)}{N_e(\infty)} = 2.25 \tag{23}$$

Note that the ratio is independent of the value of $\tilde{N}$ and the polymer properties ρ, l, C_∞, and μ_m and is therefore predicted to be universal.

The variation of N_e by a factor of 2.25 translates into a similar variation of the plateau modulus, with the lowest values of plateau modulus occurring at N_c. A variation of the plateau modulus, in this chain length regime, has not been reported in experimental studies. However, for chain lengths just above N_c, the plateau region is seldom observed because of its narrow width and the strong influence of polydispersity. Although the effect is not documented, a visual examination of stress–relaxation master curves[19] reveals that for lengths $N \simeq N_c$ the curves are somewhat separated in the time domain where the plateau is expected, even on a logarithmic scale. A confirmation of the effect, however, awaits further experimental investigation.

The predicted variation of entanglement spacing with chain dimensions has greater consequences for the zero shear viscosity where the entanglement spacing appears as a squared quantity. According to reptation theory[1,2] or a generalized Rouse model,[15,16] the zero shear rate viscosity scales with degree of polymerization and entanglement spacing according to

$$\eta_o \propto N^3/N_e^2 \tag{24}$$

In our entanglement model, N_e is given by the complicated function in eq 8 and does not lead to a simple scaling correction to the 3.0 power law. If, however, we insist in representing eq 24 in a scaling law form, the appropriate expression is

$$\eta_o \propto N^{3+\delta(N)} \tag{25}$$

where the scaling correction function $\delta(N)$ varies continuously from about $^1/_2$ for $N \simeq N_c$ to 0 for higher N. The function $\delta(N)$ decays to 0 over a wider range of N values because of the squared term in the denominator of eq 24. Since N_e is predicted to be larger by a factor of 2.25 at N_c, the zero shear viscosity is therefore lower by about a factor of 5, than predicted by traditional reptation theory.

Equations 8 and 24 therefore predict that the entanglement variation contributes to the deviation from reptation theory in much the same way as the Doi's length fluctuations.[5] That is, the deviations persist over about $1^1/_2$ decades of molecular weight but disappear for higher molecular weight. Unlike the fluctuations approach, we have not introduced a new parameter to adjust the magnitude of the effect. In fact, we have reduced the number of parameters in the problem by replacing N_e by a relation containing measurable material parameters and a constant which is universal. Fluctuation phenomena can also be incorporated into the entanglement model and would probably smoothen the transition and extend the width of the transition as in the liquid–gas problem.

Recent measurements by Colby et al.[20] on polybutadiene have suggested that departures from reptation theory, the zero shear viscosity, may be limited to a narrow range above N_c. They chose polybutadiene because of its low entanglement molecular weight, M_e = 1850, and determined that the zero shear viscosity deviation from the 3.0 scaling law persists for about $1^1/_2$ decades of molecular weight and suggested that the reptation theory results may be valid beyond this.

In Figure 4 we have plotted the raw data on polybutadiene from Colby et al.[20] and a continuous curve computed from eq 8 and 24. In computing this curve, we used the mean value of $\tilde{N}$ and material parameters from Table I. The viscosity values were divided by M^3 to remove the pure reptation component. Any nonzero slope here therefore represents a departure from reptation theory. The first 12 points on the plot correspond to chains with $M < M_c$, hence the negative slope. The computed curve of η_o/M^3 varies sufficiently to account for the magnitude of the deviation from pure reptation, but the fit is somewhat poor. The data vary more slowly than the computed curve. We can only speculate that this is partly due to the mean field nature of the model and specifically the absence of fluctuations which become more important near the transition as well as the absence of a renewable process. We comment further on this in section 5.

The variation of N_e with what we have predicted also has the same consequences for the self-diffusion coefficient since $D_{self} \propto N_e/N^2$, from the reptation theory.[1] However, since N_e appears in the numerator to the first power, rather than squared power as it appears in the denominator of eq 24 for the viscosity, the scaling law correction is less significant. For example, a viscosity scaling law of $\eta_o \propto N^{3.4}$ in the crossover region would imply a self-diffusion

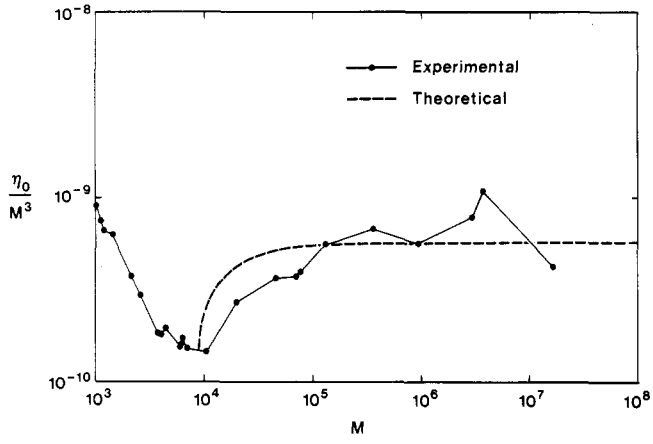

Figure 4. Zero shear viscosity, η_0, as a function of molecular weight, M, of polybutadiene as reported by Colby et al.[20] The data in this plot have not been corrected to the isofree volume state. The viscosities are reduced by M^3 in order to remove any pure reptation component. Therefore, any nonzero slope represents a departure from reptation theory. The negative slope of about −2 for the first dozen points corresponds to the Rouse regime ($M < M_e$) where the reptation theory is not applicable. Beyond M_e, a positive slope of approximately 0.4 extends for about $1^1/_2$ decades and then levels off to zero slope, although the data are somewhat oscillatory here. The theoretical curve expresses the departure from reptation theory predicted from our entanglement model where N_e has the molecular weight dependence of eq 8. This curve was computed using the mean value of $\bar{N}$ = 8.1 and the polymer properties from Table I. The magnitude of the effect predicted by the theoretical curve is in agreement with the data. The fit in the transition region is somewhat poor. In this region, the theoretical curve varies more rapidly than the experimental data, which like other mean field theories is due to the absence of fluctuation phenomena.

scaling law of $D_{self} \propto N^{-2.2}$. This scaling law is predicted to be limited to the crossover region, $N \geq N_c$, where entanglement effects first appear. For longer chains, the model predicts that N_e is independent of chain length, and therefore the usual reptation theory prediction of $D \propto N^{-2}$ is recovered.

The predictions for the diffusion coefficient appear to be at variance with the experimental results of several groups,[28-30] where $D \propto N^{-2}$ has been reported for all N greater than N_c. More recently, other groups have reported experimentally determined power laws of the form $D \propto N^{-a}$ with a ranging from values of 2.4[31] to perhaps as high as 3.0.[32] More interestingly, the group[31] reporting the value $a = 2.4$ has suggested that this exponent applies to a limited range in molecular weight and a value of $a = 2.0$ holds for higher molecular weight. It is clear, however, that the experimental community has not yet reached a consensus of opinion on this matter and that more experimental studies are needed to fully resolve the issue. In any event, the difference between 2.0 and 2.2 is difficult to resolve on a log–log plot given the various uncertainties introduced by polydispersity, molecular weight determinations, and free volume effects.[9]

3c. The Transition at N_c. The onset of molecular entanglement phenomena can be probed experimentally in many different ways. For example, a plot η_0/M^3 versus M, as shown in Figure 4 for polybutadiene, exhibits a change in slope at the molecular weight M_c. The location of M_c, determined in this fashion, is typically in the range $2M_e$–$3M_e$, although some polymers, such as the methacrylates, yield larger values of about $6M_e$.[9] Determination of M_c in this manner is subject to a number of uncertainties, which Graessley[9] has discussed. For example, viscosity measurements are frequently made at different temperatures for different molecular weigths, and therefore the data must be corrected to a common segmental friction coefficient. this process requires knowing the temperature dependence of the viscosity for each molecular weight studied. This information is often not known or imprecise and is also subject to an imperical analysis. The data in Figure 4 have not been adjusted in this fashion and yield a value of M_c that is higher by a factor of 2–3 than the value that Colby et al.[20] reported for adjusted data.

In Figure 4 we also notice that the turning point at M_c is not very abrupt. Researchers often use the extrapolation between limiting models, such as the Rouse and reptation models, to define M_c. The procedure may further bias the value of M_c depending on the correctness of the dynamic models. Finally, the molecular weight and viscosity determinations are also subject to errors.

An alternative method of observing the onset of entanglement effects is to measure the molecular weight dependence of the creep compliance.[8] Above the entanglement molecular weight, the creep compliance exhibits a rubbery plateau, J_e^0, which is associated with a transient entanglement network. This method yields larger values than those determined from the viscosity and are often denoted as M_c'. Values of M_c' determined in this manner are typically $\sim 7M_e$. Apart from experimental uncertainties, the major drawback of this method is the high sensitivity of J_e^0 to polydispersity.[9,21]

Table II
Entanglement Parameters[a]

	M_e	M_c	M_c/M_e	M_c'	M_c'/M_e
polystyrene	18100	31200	1.7	130000	7.2
poly(α-methylstyrene)	13500	28000	2.1	104000	7.7
1,4-polybutadiene	1900	5900	3.1	13800	7.3
poly(vinyl acetate)	12000	24500	2.0	86000	7.2
poly(dimethyl-siloxane)	8100	24400	3.0	61000	7.5

[a] Data from ref 9. M_c values are extrapolated from viscosity measurements, M_c' values are from steady-state compliance measurements, and M_e values are from plateau modulus measurements.

In Table II we list the values of M_e, M_c, and M_c' for a number of polymers. The ratios of M_c/M_e and M_c'/M_e show average values of 2.4 and 7.4, respectively, with less scatter in the ratio M_c'/M_e. The origin of the difference between M_c and M_c', and therefore the quantities N_c and N_c', has been discussed in the literature[9] but has still not been fully resolved.

The entanglement theory developed in section 2 predicts a single transition at a value N_c that satisfies the two relations

$$N_c = 3N_e(N_c) \tag{26}$$

$$N_c = \frac{27}{4}N_e(\infty) \tag{27}$$

Recall that the model predicts that N_e has a molecular weight dependence around N_c, but not a higher molecular weight. Experimentally reported values of M_e and, therefore, N_e are largely derived from high molecular weight materials, where a plateau modulus is more readily extracted from experimental data. Therefore, our prediction of the ratio N_c/N_e or M_c/M_e is

$$N_c/N_e = 6.75 \tag{28}$$

which is close to the values of M_c'/M_e determined from the steady-state compliance measurements. The average experimentally determined ratio is about 7.4, which is not significantly higher than 6.75. One also expects that the reported values should be slightly higher since the method of determining N_c' is essentially to increase the molecular

weight until a plateau region is observed. This will tend to overshoot the value of N_c' by a small amount.

The present theory offers no explanation for the difference between M_c and M_c'. However, since the ratio of M_c'/M_e has little scatter as compared to M_c/M_e, it makes M_c'/M_e a more attractive quantity from the theoretical standpoint. The variation in the ratio M_c/M_e suggests that perhaps we should reevaluate the methods used to determine M_c. Recall that the determination of M_c involves both an adjustment of the friction coefficient and an interpolation between limiting dynamical models, both of which are continually being refined. The estimation of M_c' can be accomplished without reference to a dynamic model and in principle should be a more reliable estimate of when entanglement effects appear in the rheology of the material.

4. Entanglement Scaling in Solutions

In this section, we generalize our entanglement model to solutions of long, linear chain polymers. Generally, solvents are classified as either good, poor, or ideal. Poor solvents will precipitate polymer in concentrated solutions and are therefore not of direct interest in discussing entanglement effects. However, a rapid precipitation process may produce a topological disorder that differs from the equilibrium situation. The classifications good and ideal often refer to dilute polymer solutions where the scaling laws for the polymer radius of gyration with chain length differ:

$$R_g^{\text{ideal}} \propto N^{1/2} \tag{29}$$

$$R_g^{\text{good}} \propto N^{3/5} \tag{30}$$

In concentrated solutions and polymer melts, the situation is somewhat more complicated because of the increase in monomer interactions. In the high-density limit, where one has a polymer melt, the conformations are known to be ideal, that is, the *large-scale* properties obey Gaussian statistics. This surprising result can be explained several ways[22] and is now known as Flory's theorem.[23] The result presumably holds for concentrated solutions as well, but it is not clear precisely under what solution conditions it breaks down, although it is generally believed to hold when chains are strongly overlapped.[22] The remainder of this section is organized into three parts. The first deals with the generalization of our entanglement model to general solvents. The remaining two sections discuss two special situations, the concentrated θ solvent regime and the semidilute regime.

4a. General Solvents. In order to generalize our entanglement model to polymer solutions, we note that, in the most general solution situations, the radius of gyration of the polymer may depend on both the polymer density and the temperature. Similarly, the mean end-to-end distance of a subsection of polymer with N_e bonds, D_e, will depend on density, temperature, and, of course, N_e. Following our previous work,[15,16] we inscribe a subsection of polymer with N_e bonds, in a sphere with volume $V_e = (\pi/6)D_e^3$, and write

$$\frac{\pi}{6}\rho_m D_e^3 = N_e + \sum_{m=1}^{N} N(m)m \tag{31}$$

The product of the left-hand side represents the mean number of monomers in volume V_e. The first term on the right-hand side is the contribution to $\rho_m V_e$ from the test chain, and the second term is the contribution due to all other chains. The function $N(m)$ is the mean number of other polymer segments in volume V_e with exactly m bonds. Again, following the development in ref 15 and 16, we can rewrite the last equation as

$$\tilde{N} + 1 = \frac{\pi\rho_m D_e^3}{6N_e}(1 - N_e/N) \tag{32}$$

where the coordination number, $\tilde{N}$, is the mean number of nontail neighboring polymers that define the entanglement and is given by

$$\tilde{N} = \frac{1}{N_e}\sum_{m=1}^{N} N_{\text{nontails}}(m)m \tag{33}$$

where $N_{\text{nontails}}(m)$ is the distribution of nontail segments in the volume. Equation 32 reduces to eq 2 by substituting $D_e = C_\infty^{1/2}N_e^{1/2}l$, which is appropriate for Gaussian chains in a melt.

We can continue the general discussion assuming that the polymer dimensions, on the entanglement length scale, can be described by a function of the form

$$D_e = C(\rho,T)N_e^a l \tag{34}$$

where C is a function that in general will depend on density and temperature and a is a scaling exponent. Equation 34 can be viewed as a definition for the function C. In the most general situation, both C and a will depend on the solvent as well. Substituting these definitions into eq 32, we obtain a generalization of eq 2:

$$\tilde{N} + 1 = \pi\rho_m C(\rho,T)^3 N_e^{3a-1} l^3 (1 - N_e/N)/6 \tag{35}$$

The scaling properties of the entanglement spacing with density cannot be specified from eq 35 without a model for the function $C(\rho,T)$ and the exponent a, which is beyond the scope of the present work. We can, however, extract some of the density dependence of N_e for special cases. For example, in the long-chain limit, the second term on the right-hand side of eq 35 vanishes and we have

$$\tilde{N} + 1 = \pi\rho_m C(\rho,T)^3 N_e^{3a-1}(\infty) l^3/6 \tag{36}$$

or rearranging we have

$$N_e(\infty) = \left[\frac{6(\tilde{N}+1)}{\pi\rho_m C(\rho,T)^3 l^3}\right]^{1/(3a-1)} \tag{37}$$

$$N_e(\infty) \propto \rho_m^{-(1/(3a-1))} C(\rho,T)^{-(3/(3a-1))} \tag{38}$$

For some special solution regimes, the function $C(\rho,T)$ is known from previous work. In the next two sections, we consider the special limiting cases of concentrated θ solutions and semidilute solutions

$$N_e \propto \rho_m^{-2} \tag{39}$$

$$N_e \propto \rho_m^{-5/4} \tag{40}$$

respectively.

4b. Concentrated θ Solutions. Here we consider a special situation of a concentrated θ solution. Here the standard assumption is that the polymer conformations are ideal or Gaussian for *all* length scales larger than the Kuhn length. The mean entanglement diameter, D_e, in eq 34 is therefore

$$D_e = C_\infty^{1/2} N_e^{1/2} l \tag{41}$$

where C_∞ is the characteristic ratio and is assumed to be independent of temperature and density. This reduces the relationship between N_e and the topological constant, $\tilde{N}$, to the same form as eq 2

$$\tilde{N} + 1 = \left(\frac{\pi\rho C_\infty^{3/2} l^3}{6\mu_m}\right) N_e^{1/2}(1 - N_e/N) \tag{42}$$

where ρ, the monomer mass density, is our concentration variable. Note that with the addition of solvent we eventually would reach the semidilute regime, where the assumption in eq 41 breaks down. We disregard this for the moment and proceed to develop scaling laws for this model system. In section 4c, we discuss the semidilute regime where the large-scale properties are Gaussian but the small-scale properties are perturbed relative to the melt.

With eq 42, we can investigate the concentration dependence of the mean entanglement spacing, N_e. The presence of the second quantity in parentheses on the right-hand side of eq 42 will lead to a transition to an unentangled state, similar to the analysis in section 2. In this case, the addition of solvent, beyond a certain critical amount, will result in a system where the entanglement criterion, of having $\tilde{N}$ neighboring segments per entanglement, is not met. For the remainder of this subsection, we will assume a fixed polymer degree of polymerization, N, that is greater than the critical chain length for entanglements, N_c, in a pure melt. We will also assume that the polymer's conformational statistics are Gaussian for all concentrations.

For very long chains, $N \gg N_c$, and concentrated solutions, the second quantity in parentheses on the right-hand side of eq 42 can be ignored, and we obtain a simple scaling relationship between N_e and ρ

$$N_e = \left[\frac{6(\tilde{N}+1)\mu_m}{\pi C_\infty^{3/2} l^3}\right]^2 \frac{1}{\rho^2} \tag{43}$$

$$N_e \propto 1/\rho^2 \tag{44}$$

where the bracketed constant is independent of both temperature and density. Since N_e is growing rapidly with decreasing density, the assumption that $N \gg N_e$ breaks down and the scaling of N_e with ρ deviates from the form expressed in eq 43. At lower density still, we approach a strong deviation from $N_e \propto \rho^{-2}$ scaling as we reach a lower critical density, ρ_c. Below ρ_c, the chains in solution are unentangled.

The function $N_e(\rho)$ is also a function of the chain length, N. For example, long chains ($N \gg N_c$) will be entangled over a wider range of density than short chains ($N \simeq N_c$). We can compute the concentration threshold for entanglements as follows. Recall that, for a pure melt, the critical chain length for entanglements (eq 22 and 43) is

$$N_c = 3^5[(\tilde{N}+1)\mu_m/\pi\rho C_\infty^{3/2} l^3]^2 \tag{45}$$

For chains with $N > N_c$, we can use this relation to compute the density at which a chain with degree of polymerization N is a critical chain length for entanglements. Therefore, substituting $N = N_c$ and $\rho = \rho_c$ into eq 45 and rearranging for ρ_c, we obtain

$$\rho_c = \left[\frac{3^{5/2}(\tilde{N}+1)\mu_m}{\pi C_\infty^{3/2} l^3}\right] N^{-1/2} \tag{46}$$

$$\rho_c \propto N^{-1/2} \tag{47}$$

This last result parallels the development by de Gennes[22] for the overlap of polymer chains in Θ solvents. He showed that the overlap threshold, $\rho_{o.c.}$, scaled with chain length, N, as

$$\rho_{o.c.} \propto N^{-1/2} \tag{48}$$

In our developments, we have imposed the stronger criterion that the chains are entangled and not simply overlapped. The entanglement threshold is therefore expected to be larger than the overlap threshold. The fact that the two scaling laws are similar is, however, not too surprising, since we can choose a lower value of $\tilde{N}$ (of say $\tilde{N} = 1$) in eq 46 to correspond to an overlap criterion rather than an entanglement criterion. With the previous argument, we can relate the two concentration thresholds, for entanglement and overlap, according to

$$\rho_c/\rho_{o.c.} \approx (\tilde{N}+1)/2 \tag{49}$$

which, like eq 28, is predicted to be a universal ratio.

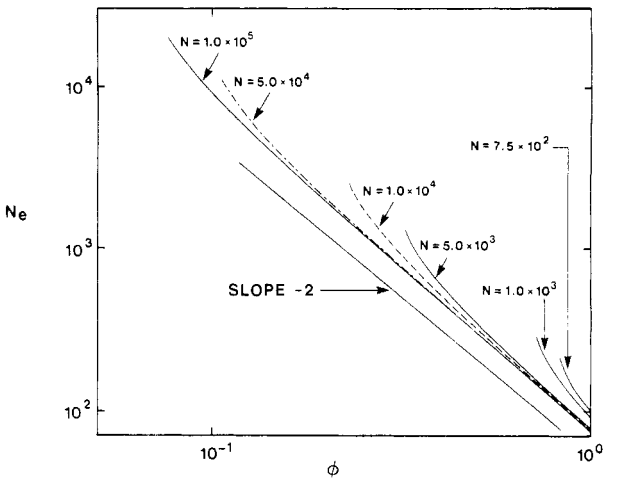

Figure 5. Mean entanglement spacing, N_e, versus polymer volume fraction, ϕ, for various degrees of polymerization and Θ solvent conditions. The curves were computed by using eq 50 and the values $\tilde{N} = 8.1$ and $C_\infty^{3/2} l^3/\mu_m = 2$. These curves exhibit an asymptotic polymer density dependence of $N_e \propto \rho^{-2}$ with departures from this form as the density is lowered toward $\rho_c = [(3^{5/2}(\tilde{N}+1)\mu_m)/(\pi C_\infty^{3/2} l^3)]N^{-1/2}$. Below ρ_c and the corresponding value of ϕ_c, the solution is unentangled. The concentration threshold for entanglements is $(\tilde{N}+1)/2 \approx 4.5$ times greater than the overlap threshold. The high density limits of the N_e curves are different for the various chain lengths, as is discussed in section 2, but the differences are small for the largest chains.

Having computed ρ_c for this system, we can now make use of eq 8 to write down the exact solution of the function $N_e(\rho,N)$. For $\rho > \rho_c$ and $N > N_c$, we have

$$N_e(\rho,N) = 4/3N \cos^2 [(1/3) \arccos (\rho_c/\rho) + 4\pi/3] \tag{50}$$

where ρ_c is given by eq 46 and contains additional N dependence. In Figure 5 we plot a family of curves, computed from this relation, each with a different value of N. The curves show the $N_e \propto \rho^{-2}$ scaling, from eq 43, in the high-density regime with departures from this scaling law as their respective values of ρ_c are approached from above. The critical behavior of $N_e(\rho)$ is analogous to the critical behavior of $N_e(N)$. Expanding the exact solution in eq 50 around $\rho = \rho_c$, we obtain

$$\frac{N_e(\rho) - N_e(\rho_c)}{2N_e(\rho_c)} = -3^{1/2}\frac{(\rho^2 - \rho_c^2)^{1/2}}{\rho_c} \tag{51}$$

$$\frac{N_e(\rho) - N_e(\rho_c)}{2N_e(\rho_c)} \approx -6^{1/2}\left(\frac{\rho - \rho_c}{\rho_c}\right)^{1/2} \tag{52}$$

which, like $N_e(N)$, has the mean field, or classical exponent, $\delta = {}^1/_2$.

Having identified a transition with ρ that is analogous to the transition that occurs with chain length, we can now discuss a "phase diagram" in the parameter space N and ρ. In Figure 6 we plot such a diagram with the entangled and unentangled regions outlined. The solid line denotes the boundary between entangled and unentangled regimes,

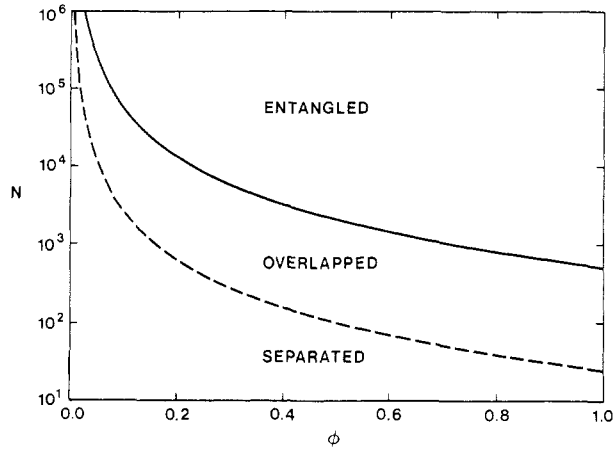

Figure 6. "Phase" diagram for polymer solutions under Θ conditions. The solid line separates the entangled and unentangled regimes. From the entangled regime, a sufficient decrease in degree of polymerization, N, or polymer volume fraction, ϕ, leads to an unentangled state. The dotted line denotes the overlap threshold, which is discussed in section 4b.

and the dotted line separates the overlapped chains regime from the separated chains regime. The line dividing the entangled and unentangled phases satisfies

$$N = 3^5\left[\frac{(\tilde{N}+1)\mu_m}{\rho C_\infty^{3/2} l^3}\right]^2 \tag{53}$$

which we used previously to define N_c for fixed ρ and ρ_c for fixed N.

4c. Semidilute Solutions. Now we turn our attention to the semidilute regime. Here the polymer volume fraction is low compared to the melt, but the polymer chains are overlapped. Of particular interest to us is the density regime where the chains are entangled and not simply overlapped. In this regime, the Flory theorem holds and the large-scale properties of the polymer are Gaussian. However, it is well-known from neutron scattering studies on polystyrene solutions[24] that the short length scale correlations are similar to those of single chains in good solvents. Therefore, the conformations are perturbed on short length scales but ideal on longer length scales. Daoud[24] showed that, in this regime, the mean squared end-to-end distance of chains is swollen relative to the pure melt and can be described by the relation

$$\langle R^2 \rangle = C_\infty N l^2 \phi^{-1/4} \tag{54}$$

where ϕ here is the polymer volume fraction. He verified this result by measuring the radius of gyration of polystyrene in solutions covering 10^{-2}–1.0 g/cm^3 and found good agreement with eq 54 in the entire range of concentrations.

In an entangled system, the entanglement length scale, D_e, is sufficiently large to incorporate the interactions between many chains. Therefore, on this length scale, the conformational statistics are also assumed to be Gaussian, and we use the developments in the last section for Gaussian chains, with one important modification. The characteristic ratio, C_∞, which we had previously assumed to be independent of density, now includes the density dependence of eq 54

$$D_e = C_\infty^{1/2}(\phi) N_e^{1/2} l \tag{55}$$

where

$$C_\infty(\phi) = C_\infty(1)\phi^{-1/4} \tag{56}$$

and $C_\infty(1)$ refers to the melt. The effect of solvent here is therefore to swell the Kuhn length.

Substituting the last two equations into eq 32, we can relate the entanglement spacing N_e to $\tilde{N}$ as follows

$$\tilde{N} + 1 = \left[\frac{\pi\rho C_\infty(1)^{3/2} l^3}{6\mu_m \phi^{3/8}}\right] N_e^{1/2}(1 - N_e/N) \tag{57}$$

and therefore in the long-chain limit ($N_e/N \ll 1$) the entanglement spacing is

$$N_e = \left[\frac{6(\tilde{N}+1)\mu_m}{\pi C_\infty^{3/2}(1) l^3}\right]^2 \frac{\phi^{3/4}}{\rho^2} \tag{58}$$

Since, $\phi \propto \rho$, the entanglement density scales with N_e according to

$$N_e \propto \rho^{-5/4} \tag{59}$$

This leads to the following scaling law prediction for the plateau modulus:

$$G_N^0 \propto \rho^{9/4} \tag{60}$$

which is in good agreement with experiments[9] where the scaling exponents is in the range 2.0–2.3.

Similarly, the critical chain length for entanglements will scale with density according to

$$N_c \propto (\tilde{N}+1)^2 \rho^{-5/4} \tag{61}$$

This prediction agrees with earlier predictions by de Gennes[26] and Klein.[27] The concentration threshold for entanglements, ρ_c, therefore scales with chain length as

$$\rho_c \propto (\tilde{N}+1)^{8/5} N^{-4/5} \tag{62}$$

The density scaling of N_e is an asymptotic result, and departures from this relation, tending to a more negative exponent, are expected as the solution density decreases toward ρ_c.

The critical concentration, ρ_c, for entanglements in semidilute systems parallels the results by de Gennes[22] for overlap density, ρ^*, in semidilute systems where he found

$$\rho^* \propto N^{-4/5} \tag{63}$$

Using our entanglement model, we can also address the question of overlap by choosing a small value of $\tilde{N} \approx 1$ as an overlap criterion rather than an entanglement criterion. This leads to the prediction that ρ_c and ρ^* are related by a universal number

$$\rho_c/\rho^* \approx \left(\frac{\tilde{N}+1}{2}\right)^{8/5} \tag{64}$$

Since $\tilde{N}$ is approximately 8.1, from our analysis of melt data, the ratio ρ_c/ρ^* is predicted to be approximately 11. This implies that there is a large solution regime between chain overlap and chain entanglement. A diagram showing the entangled and overlapped regimes as a function of concentration and chain length is shown in Figure 7.

Recent experimental data on polystyrene solutions[25] support our prediction in eq 64. This study found that ρ_c/ρ^* is approximately 10. More importantly, these data did suggest a molecular weight independence of this ratio, in agreement with eq 64. The question of the universality of this ratio awaits similar experimental studies on different polymers.

It is interesting to note that we could have arrived at eq 63 by assuming that the conformations are perturbed, as in the single chain in good solvent, on the entanglement length scale. This would have involved choosing

$$D_e = C N_e^{3/5} l \tag{65}$$

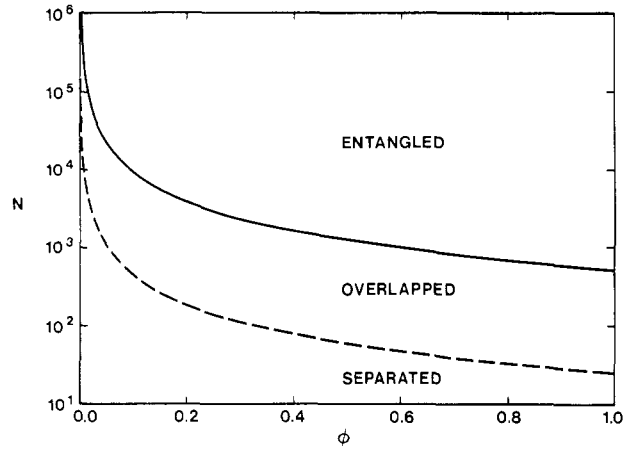

Figure 7. "Phase" diagram for polymer solutions under good solvent or semidilute conditions. Here the solid line separates the entangled/unentangled regimes. N is the degree of polymerization and ϕ is the polymer volume fraction. The dotted line denotes the overlap threshold, which is discussed in section 4c.

and substituting this into eq 32. This assumption, however, could only apply to very dilute systems, which are presumably not entangled.

5. Summary and Conclusions

The purpose of this paper was to develop scaling laws for molecular entanglements in polymer melts and solutions and to compare these predictions against experimental data. The scaling laws were derived from a model of chain entanglements[15,16] which describes an effective entanglement as consisting of a certain number, $\tilde{N}$, of neighboring, nontail, polymer segments. The number, $\tilde{N}$, which we call the coordination number and conjecture its universality in both melts and solutions, represents the number of neighboring chains that on the average, or in a mean field manner, restrict the lateral degrees of freedom of a test chain. The coordination number along with the relevant polymer properties (C_∞, l, μ_m, and N) predict the value of N_e. The model also predicts a value for N_c for a given polymer and described a transition to the unentangled state as being analogous to the liquid–gas critical point. A one-to-one correspondence between our entanglement model and the van der Waals equation of state was demonstrated in section 2.

In section 3a, we compared our predictions of N_e for various polymers and found a high degree of correlation between the predicted expression

$$N_e = \left[\frac{6(\tilde{N}+1)\mu_m}{\pi\rho_m C_\infty{}^{3/2} l^3}\right]^2 \tag{66}$$

and the experimental data. The experimental data yielded a average value of $\tilde{N} = 8.1$. The small scatter in $\tilde{N}$ supports our conjecture that $\tilde{N}$ is universal.

The transition to the unentangled state was discussed in section 3b. In this regime, our model predicts that the entanglement spacing, N_e, varies with molecular weight in a manner that has important consequences for rheological properties. For example, the zero shear viscosity scaling law departures from reptation theory can in part be explained by this effect. Quantitative agreement with experimental data was not obtained in this situation. This, however, is not too surprising, given that the entanglement model is a mean field model with the absence of fluctuations. In general, the transitions predicted by mean field theories are more abrupt than those observed. The overall magnitude of the departure from reptation theory is in good agreement with the experimental results. A minor molecular weight dependence was predicted for the plateau modulus near the unentangled transition. There is, however, insufficient data in the literature to test this prediction.

Our predictions for the location of the entangled–unentangled transition at N_c and particularly the ratio $N_c/N_e = 6.75$ are in good agreement with data derived from creep compliance experiments but not in good agreement with the values determined from viscosity data. In section 3c, we speculate as to the possible reasons for this discrepancy but don't feel that the issue has been resolved.

In section 4 we generalized the entanglement model to polymers in solution. Here we derived scaling laws for the entanglement spacing as a function of polymer density for a very general solvent. Specific predictions were made for Θ solvents and semidilute solutions. For the semidilute regime, we predict that the density dependence of the entanglement spacing and plateau modulus are as given in eq 59 and 60, respectively. The latter scaling law is in good agreement with experimental data[9] where $G_N^\circ \propto \rho^a$ with $a \approx 2$–2.3. For Θ solvents, we predict that the density dependence of the entanglement spacing and plateau modulus are

$$N_e \propto \rho^{-2} \tag{67}$$

$$G_N^\circ \propto \rho^3 \tag{68}$$

respectively. At present, data on entangled systems in Θ solvents are somewhat scarce. The recent studies by Adam and Delsanti[33] on polystyrene in cyclohexane have found that the shear elastic modulus varies as $G_N^\circ \propto \rho^\beta$, where the exponent β was found to be $\beta = 2.5 \pm 0.2$. While this value is somewhat larger than the range reported for good solvents,[9] it is not as large as the 3.0 value predicted in the present paper. The data of Adam and Delsanti,[33] however, only cover a limited concentration range (0.02–0.10 g/cm^3). A series of experiments covering a wider concentration range is needed in order to determine the scaling exponent more precisely. It is interesting to note that the scaling exponent for the bulk modulus[33] is 3.0 for the concentration range mentioned above.

To summarize, a relatively simple description of entanglements has provided us considerable insight into an otherwise complex topological problem. Without invoking dimensional analysis type arguments, we derived several scaling laws, complete with numerical coefficients, that relate the microscopic properties of polymers to the rheological properties that are influenced by chain entanglements. The contact that we made with the analogous liquid–gas critical point may offer some guidance for improving the model further.

Acknowledgment. The authors thank Professor P.-G. de Gennes for his insightful comments and pointing out the large solution regime that our model predicts between overlapped chains and entangled chains. T. A. Kavassalis thanks the Natural Science and Engineering Research Council of Canada for financial support in the form of an industrial research fellowship.

Registry No. Polystyrene, 9003-53-6; poly(α-methylstyrene), 25014-31-7; polybutadiene, 9003-17-2; polyisobutylene, 9003-27-4; polyisoprene, 9003-31-0; poly(vinyl acetate), 9003-20-7; polyethylene, 9002-88-4.

References and Notes

(1) de Gennes, P. G. *J. Chem. Phys.* **1971**, *55*, 572.
(2) Doi, M.; Edwards, S. F. *J. Chem. Soc., Faraday Trans. 2* **1978**, *74*, 1789, 1802, 1818.
(3) Edwards, S. F. *Proc. Phys. Soc., London* **1967**, *92*, 9.
(4) Graessley, W. W. *Adv. Polym. Sci.* **1982**, *47*, 67.
(5) Doi, M. *J. Polym. Sci., Polym. Lett. Ed.* **1981**, *19*, 265.

(6) Des Cloizeuax, J. *J. Phys.* (*Les Ulis, Fr.*) **1984**, *45*, 1–17.
(7) Hess, W. *Macromolecules* **1987**, *20*, 2587.
(8) Ferry, J. D. *Viscoelastic Properties of Polymers*; Wiley: New York, 1980, and references contained within.
(9) Graessley, W. W. *Adv. Polym. Sci.* **1974**, *16*, 1.
(10) Fox, T. G.; Allen, V. R. *J. Chem. Phys.* **1964**, *41*, 344.
(11) Privalko, V. P. *Macromolecules* **1980**, *13*, 370.
(12) Graessley, W. W.; Edwards, S. F. *Polymer* **1981**, *22*, 1329.
(13) Aharoni, S. H. *Macromolecules* **1983**, *16*, 1722; **1986**, *19*, 426.
(14) Lin, Y.-H. *Macromolecules* **1987**, *20*, 3080.
(15) Kavassalis, T. A.; Noolandi, J. *Phys. Rev. Lett.* **1987**, *59*, 2674.
(16) Kavassalis, T. A.; Noolandi, J. *Macromolecules* **1988**, *21*, 2869.
(17) Flory, P. J. *Chem. Rev.* **1944**, *35*, 51.
(18) Stanley, H. E. *Introduction to Phase Transitions and Critical Phenomena*; Oxford University Press: Oxford, 1971, and references contained within.
(19) Onogi, S.; Masuda, J.; Kitagawa, K. *Macromolecules* **1970**, *3*, 109.
(20) Colby, R. H.; Fetters, L. J.; Graessley, W. W. *Macromolecules* **1987**, *20*, 2226.
(21) Struglinski, M. J.; Graessley, W. W. *Macromolecules* **1985**, *18*, 2630.
(22) de Gennes, P. G. *Scaling Concepts in Polymer Physics*; Cornell University Press: Ithaca, NY, 1979.
(23) Flory, P. J. *J. Chem. Phys.* **1949**, *17*, 303.
(24) Daoud, M. *Macromolecules* **1975**, *8*, 804.
(25) Nemoto, N.; Okada, S.; Inoue, T.; Kurata, M. *Macromolecules* **1988**, *21*, 1502.
(26) de Gennes, P. G. *Macromolecules* **1976**, *9*, 594.
(27) Klein, J. *Macromolecules* **1978**, *11*, 852.
(28) Klein, J. *Nature* (*London*) **1978**, *271*, 143.
(29) Leger, L.; Hervet, H.; Rondelez, F. *Macromolecules* **1981**, *14*, 1732.
(30) Green, P. F.; Palmstrom, C. J.; Mayer, J. W.; Kramer, E. J. *Macromolecules* **1985**, *18*, 501.
(31) Antonietti, M.; Coutandin, J.; Sillescu, H. *Macromolecules* **1986**, *19*, 793.
(32) Kim, H.; Chang, T.; Yoharan, J. M.; Wong, L.; Yu, H. *Macromolecules* **1986**, *19*, 2737.
(33) Adam, M.; Delsanti, M. *J. Phys.* (*Les Ulis, Fr.*) **1984**, *45*, 1513.

Immobilization of Transient Structures in Polystyrene/Poly(2-chlorostyrene) Blends Undergoing Phase Separation by Using Photo-Cross-Linking

Q. Tran-Cong,* T. Nagaki, T. Nakagawa, O. Yano, and T. Soen

Department of Polymer Science and Engineering, Kyoto Institute of Technology, Matsugasaki, Kyoto 606, Japan. *Received December 27, 1988; Revised Manuscript Received March 24, 1989*

ABSTRACT: Immobilization of the transient phase-separated structures during the spinodal decomposition process in the polystyrene/poly(2-chlorostyrene) blend is demonstrated by taking advantages of photo-cross-linking via photodimerization of anthracene moieties chemically attached to polystyrene chains. For this purpose, anthracene-labeled polystyrene (PSA)/poly(2-chlorostyrene) (P2CS) blends of composition (41.4/58.6) were jumped from the one-phase region into the spinodal region and were subsequently irradiated by UV light from a high-pressure mercury (Hg) lamp (365 nm) and a XeF excimer laser (351 nm). During the time evolution of the spinodal decomposition, cross-linking between different segments of PSA takes place via intermolecular photodimerization of anthracene groups. By dielectric measurements, it is found that there is a remarkable difference in tan δ between these irradiated blends and another of the same composition carried out without UV irradiation under the same thermal conditions. The morphology of the blend irradiated by a Hg lamp shows that the spinodal-like structures were partially immobilized, whereas these specific structures were frozen efficiently upon irradiation with a XeF excimer laser. These preliminary results reveal the possibility of designing new polymer blends with ordered structures in the range of micrometers by photo-cross-link.

Physical properties of polymer blends strongly depend on their structures at the molecular level resulting from the phase separation process. It is expected that immobilization of the transient structures in polymer blends undergoing a phase decomposition process would provide materials with unique properties due to the spatial concentration distributions of both component polymers. In fact, the time evolution characteristics of these transient structures determined by the kinetics of phase decomposition processes have been extensively investigated in recent years.[1-5] For the lower critical solution temperature (LCST) type polymer blends which undergo phase separation upon heating, the simplest way to immobilize these transient phase-separated structures is quenching quickly the blend undergoing phase separation at high temperatures to temperatures much lower than the glass transition temperatures of both components. However, the molecular structures obtained in this way are not permanently fixed due to the molecular motions in the vicinity of T_g and, particularly, to the polymer chain diffusion at high temperatures. Consequently, it is difficult to investigate the structure/properties relationships in these frozen materials.

In this paper, we would like to report some preliminary experimental results on immobilization by photo-cross-linking the transient structures in polystyrene/poly(2-chlorostyrene) blends obtained by temperature jump (T-jump) from the one-phase region into the spinodal unstable region. The cross-linking is achieved by taking advantages of intermolecular photodimerization of anthracene groups[6] chemically attached on polystyrene chains upon UV irradiation.

The structures of the component polymers are shown in Figure 1. Anthracene-labeled polystyrene (PSA, M_w = 140 000, M_w/M_n = 1.9) is prepared by Williamson synthesis from chloromethylated polystyrene and 9-anthracenemethanol (Aldrich, recrystallized) by the procedure described previously.[7] The average labeling ratio for polystyrene is 11 anthracene groups per chain. Poly-

* To whom correspondence should be addressed.

0024-9297/89/2222-2720$01.50/0